University of Illinois at Urbana-Champaign

Degree of Doctor of Physics

Drell-Yan at COMPASS rocks it!

Candidate: Robert Shannon Heitz

Supervisor: Prof. Matthias Grosse-Perdekamp

Supervisor: Prof. Caroline Riedl

To whom it may concern

Abstract

Dear Barbara Badelek, hereafter my abstract

Table of Contents

Chapter 1

Measurement of the Left-Right Asymmetry in the Drell-Yan Process

Introduction about L/R asym. In this Chapter.... Define AN

1.1 Data Sample

The data sample comes from the 2015 COMPASS Drell-Yan measurement where a 190 GeV/c π^- beam impinged on a transversely polarized NH_3 target. The stable data comes from July 8, through November 12 and is split into 9 periods lasting approximated 2 weeks each where each period consist of two sub-periods. To reduce systematics, the NH_3 target was split into two oppositely polarized cells with one cell polarized up and one cell polarized down. The cells were separated by 20 cm and the polarization of both cells was flipped between sub-periods. A summary of the data taking from each period is shown in table 1.1.

1.1.1 Event Selection

The cuts in the event selection were chosen to ensure the final state consisted of dimuons resulting from a pion collision in the transversely polarized target. The event selection was initial filtered from miniDSTs to μDSTs using the criteria of at least two muons in the final state. The final cuts are described in the following enumerated list where the event selection is performed on these μDSTs and the events used come from the slot1 production. A summary of the number of events remaining after each cut is shown in table 1.2.

1. Two oppositely charged particles from a common best primary vertex. A primary vertex is defined as any vertex with an associated beam particle. In case of multiple common primary vertices the best primary vertex was determined by CORAL tagging

Period	Sub-period	Polarization	First-Last run	Begin date	End date
W07	one	↓↑	259363 - 259677	July 9	July 15
	two	↑↓	259744 - 260016	July 16	July 22
W08	one	↑↓	260074 - 260264	July 23	July 29
	two	↓↑	260317 - 260565	July 29	August 5
W09	one	↓↑	260627 - 260852	August 5	August 12
	two	↑↓	260895 - 261496	August 12	August 26
W10	one	↑↓	261515 - 261761	August 26	September 1
	two	↓↑	261970 - 262221	September 4	September 9
W11	one	↓↑	262370 - 262772	September 11	September 22
	two	↑↓	262831 - 263090	September 23	September 30
W12	one	↑↓	263143 - 263347	September 30	October 7
	two	↓↑	263386 - 263603	October 8	October 14
W13	one	↓↑	263655 - 263853	October 15	October 21
	two	↑↓	263926 - 264134	October 22	October 28
W14	one	↑↓	264170 - 264330	October 28	November 2
	two	↓↑	264429 - 264562	November 4	November 8
W15	one	↓↑	264619 - 264672	November 9	November 11
	two	↑↓	264736 - 264857	November 12	November 16

Table 1.1 COMPASS 2015 data taking periods

the vertex as best primary (PHAST method PaVertex::IsBestPrimary()). In the case that CORAL did not tag any of the common vertices as the best primary the vertex with the smallest spatial chi^2 value was used as the best primary vertex.

2. A dimuon trigger fired. A dimuon trigger firing means there are at least two particles in coincidence in this event. The dimuon triggers used were a coincidence between two particles in the large angle spectrometer, LAS-LAS trigger, or a particle in the large angle spectrometer and a particle in the Outer hodoscope in the small angle spectrometer, LAS-Outer trigger. The LAS-Middle trigger was used as a veto on beam decay muons. This is because the LAS-Middle trigger was found to have many events resulting from a beam pion decaying to a muon.

3. Both particles are muons. A muon was defined as having crossed 30 radiation lengths of material between the particles first and last measured points. This criteria has been previously determined to be effective at distinguishing between muons and hadrons. In the final production no detectors were used from upstream of the hadron absorber so the absorber is not included in the determination of material crossed.

4. The first measured point for both particles is before 300 cm and the last measured point is after 1500 cm. This cut ensures both particles have positions upstream of the first spectrometer magnet and downstream of the first muon filter.

5. The timing of both muons is defined. This checks that the time relative to the trigger time is determined for both muons so further timing cuts can be performed.

6. Both muons are in time within 5 nanoseconds. This cut helps rejected uncorrelated muons.

7. The muon track's spacial reduced chi^{2}s are individually less than 10. This cut ensure track quality.

8. A validation that each muon crossed the trigger it was associated as having triggered. This trigger validation cut was performed by extrapolating (PHAST Method PaTrack::Extrapolate()) each muon track back to the hodoscopes it fired and determining if the muon crossed the geometric acceptance of both hodoscopes.

9. The event does not occur in the bad spill or run list. Many tests were performed to test the basic stability of the spectrometer and beam. The spills placed on the bad spill list were deemed to occur during unstable data taking conditions.

10. The Drell-Yan kinematics are physical. That is the beam and target x-Bjorken are between 0 and 1 and x-Feynman is between -1 and 1.

11. The transverse momentum of the virtual photon is between 0.4 and 5.0 GeV/c. The lower limit ensures azimuthal angular resolution is sufficient and the upper cut is minimal and further ensures the kinematic distributions are physical possible.

12. The vertex originated within the z-positions of the transversely polarized targets defined by the target group (-294.5< Z_{vertex} <-239.3 for the upstream target or -219.5< Z_{vertex} <-164.3 cm for the downstream target).

13. The vertex is within the radius of the target defined as 1.9 cm.

Cuts	W07	W08	W09	W10	W11	W12	W13	W14	W15	WAll
All Data	19410	19184	19654	20707	31371	23563	20561	13154	7697	175301
Good Spills	15947	14899	16217	16895	23041	20184	16026	11796	7422	142427
$0< x_\pi, x_N <1, -1< x_F <1$	15932	14886	16200	16885	23022	20171	16013	11794	7414	142317
$0.4< q_T <5(GeV/c)$	14342	13385	14609	15239	20667	18101	14365	10588	6636	127932
Z Vertex within NH_3	4256	4024	4330	4552	6369	5503	4411	3130	2028	38603
Vertex Radius < 1.9cm	4175	3950	4257	4474	6252	5414	4334	3078	1987	37921

Table 1.2 Final event selection statistics

1.1.2 Binning

The final asymmetries are measured in bins of x_N, x_π, x_F, q_T, and $M_{\mu\mu}$. The binning was determine by requiring equal statistics per physics bin. In addition, the asymmetry is determined in an integrated bin using all the final data. The final binning limits are summarized in table 1.3.

Kinematics	Lowest limit	Upper limit bin 1	Upper limit bin 2	Upper limit bin 3
x_N	0.0	0.13	0.19	1.0
x_π	0.0	0.40	0.56	1.0
x_F	-1.0	0.22	0.41	1.0
q_T (GeV/c)	0.4	0.86	1.36	5.0
$M_{\mu\mu}$ (GeV/c^2)	4.3	4.73	5.50	8.5

Table 1.3 Final binning limits

1.2 Extraction of Asymmetries

There are many ways to determine the left-right asymmetry denoted as A_N. The relevant techniques for the 2015 COMPASS setup are described and compared to ensure confidence in the final result. Sec. 1.2.1 starts with a general introduction to the notations and ideas used for all the asymmetry methods.

1.2.1 Geometric Mean

The number of physics counts, N, detected from any particular target can be written as

$$N = L * \sigma * a, \tag{1.1}$$

where L is the luminosity, σ is the cross-section to produce such an event and a is the acceptance. In simple words, the number of counts detected is the number of possible chances for an event to occur times the probability for an event to occur and that the event will be detected. To get spin-dependent counts for the left-right asymmetry, the target, polarization and left or right direction relative to the spin should be included in the counts formula. Generically this can be written

$$N^{\uparrow(\downarrow)}_{\text{target,Left(Right)}} = a^{\uparrow(\downarrow)}_{\text{target,spectrometer direction}} * L^{\uparrow(\downarrow)}_{\text{target}} * \sigma_{\text{Left(Right)}}, \tag{1.2}$$

where $^{\uparrow(\downarrow)}$ denotes the target polarization, $_{\text{target}}$ is either the upstream or downstream target $_{\text{Left(Right)}}$ is left or right of the spin direction and $_{\text{spectrometer direction}}$ denotes which side of the spectrometer the event was detected on and can be either the Jura or Saleve side.

The previous definitions of the detected counts all depend on the spectrometer acceptance. This is a problem because the spectrometer acceptance can change with time and space and therefore can be dependent on the physical kinematics which produced the event. Such dependences can cause unphysical false asymmetries in the measurement of A_N and must therefore be removed or must be included as systematic effects.

The geometric mean asymmetry method is a way to determine the left-right asymmetry without acceptance effects from the spectrometer. It is defined as

$$\frac{1}{P} \frac{\sqrt{N^{\uparrow}_{\text{up(down)stream,Left}} N^{\downarrow}_{\text{up(down)stream,Left}}} - \sqrt{N^{\uparrow}_{\text{up(down)stream,Right}} N^{\downarrow}_{\text{up(down)stream,Right}}}}{\sqrt{N^{\uparrow}_{\text{up(down)stream,Left}} N^{\downarrow}_{\text{up(down)stream,Left}}} + \sqrt{N^{\uparrow}_{\text{up(down)stream,Right}} N^{\downarrow}_{\text{up(down)stream,Right}}}}, \tag{1.3}$$

where P represents the fraction of polarized partons.

Equation 1.3 can be thought of simply as the normalized difference of left minus right counts. Left and right counts are determined relative to the target spin and are defined as

$$\text{Left}: \hat{q}_T \cdot (\hat{S}_T \times \hat{P}_\pi) > 0$$
$$\text{Right}: \hat{q}_T \cdot (\hat{S}_T \times \hat{P}_\pi) < 0, \tag{1.4}$$

where $\hat{q}_T$, $\hat{S}_T$ and $\hat{P}_\pi$ are unit vectors in the target reference frame for the virtual photon transverse momentum, the target spin and the beam pion momentum respectively.

Using Eq. 1.2 for the definition of counts, the geometric mean asymmetry is

$$\frac{1}{P}\frac{\kappa\sqrt{\sigma_{Left}\sigma_{Left}} - \sqrt{\sigma_{Right}\sigma_{Right}}}{\kappa\sqrt{\sigma_{Left}\sigma_{Left}} + \sqrt{\sigma_{Right}\sigma_{Right}}}, \tag{1.5}$$

where κ is a ratio of acceptances defined as

$$\kappa_{geomean} = \frac{\sqrt{a^\uparrow_{\text{up(down)stream,Jura}} a^\downarrow_{\text{up(down)stream,Saleve}}}}{\sqrt{a^\uparrow_{\text{up(down)stream,Saleve}} a^\downarrow_{\text{up(down)stream,Jura}}}}. \tag{1.6}$$

Here the detection side of spectrometer is specified by looking down the beam line as either Jura to mean left or Saleve to mean right. These relations of Jura is left and Saleve is right are only strictly true if the target polarization is pointing straight up or straight down in the target frame. In particular if the beam particle and the target polarization do not make a right angle in the laboratory frame this relation will no longer be strictly true but is an approximation for ease of notation.

Relation 1.5 is equal to A_N if κ is equal to one. However as stated previously, time effects can vary κ from unity. These effects are estimated through false asymmetry analysis and included in the systematics. Equation 1.3 is therefore to a good approximation an acceptance free method to determine A_N. It is also defined for the upstream and downstream targets independently and therefore can be used as a consistency check between the two targets.

The statistical uncertainty of the geometry mean is

$$\frac{1}{P}\frac{\sqrt{N^\uparrow_{\text{Left}} N^\downarrow_{\text{Left}} N^\uparrow_{\text{Right}} N^\downarrow_{\text{Right}}}}{\left(\sqrt{N^\uparrow_{\text{Left}} N^\downarrow_{\text{Left}}} + \sqrt{N^\uparrow_{\text{Right}} N^\downarrow_{\text{Right}}}\right)^2}\sqrt{\frac{1}{N^\uparrow_{\text{Left}}} + \frac{1}{N^\downarrow_{\text{Left}}} + \frac{1}{N^\uparrow_{\text{Right}}} + \frac{1}{N^\downarrow_{\text{Right}}}} \quad, \tag{1.7}$$

which reduces to $\frac{1}{P}\frac{1}{\sqrt{N}}$ in the case of equal statistics in each direction and polarization.

1.2.2 Two Target Geometric Mean

The previous method determined an A_N per target and as mentioned before COMPASS had two oppositely polarized targets in 2015. It would therefore makes sense from a statistical point of view and for comparison purposes to determine A_N using all the information from the 2015 COMPASS setup. This can be accomplished by modifying the geometric mean to add both targets as follows

$$\frac{1}{P}\frac{\sqrt[4]{N^{\uparrow}_{\text{up,Left}}N^{\downarrow}_{\text{up,Left}}N^{\uparrow}_{\text{down,Left}}N^{\downarrow}_{\text{down,Left}}}-\sqrt[4]{N^{\uparrow}_{\text{up,Right}}N^{\downarrow}_{\text{up,Right}}N^{\uparrow}_{\text{down,Right}}N^{\downarrow}_{\text{down,Right}}}}{\sqrt[4]{N^{\uparrow}_{\text{up,Left}}N^{\downarrow}_{\text{up,Left}}N^{\uparrow}_{\text{down,Left}}N^{\downarrow}_{\text{down,Left}}}+\sqrt[4]{N^{\uparrow}_{\text{up,Right}}N^{\downarrow}_{\text{up,Right}}N^{\uparrow}_{\text{down,Right}}N^{\downarrow}_{\text{down,Right}}}}, \qquad (1.8)$$

where up and down stand for the upstream and downstream targets respectfully.

As in the basic geometric mean, left and right are determined relative to the spin direction of the target as in Eq. 1.4. Again using Eq. 1.2 for the definition of counts, the two target geometric mean asymmetry, Eq. 1.8, can be written as

$$\frac{1}{P}\frac{\kappa\sqrt[4]{\sigma_{Left}\sigma_{Left}\sigma_{Left}\sigma_{Left}}-\sqrt[4]{\sigma_{Right}\sigma_{Right}\sigma_{Right}\sigma_{Right}}}{\kappa\sqrt[4]{\sigma_{Left}\sigma_{Left}\sigma_{Left}\sigma_{Left}}+\sqrt[4]{\sigma_{Right}\sigma_{Right}\sigma_{Right}\sigma_{Right}}}, \qquad (1.9)$$

,

where now κ is the ratio of acceptances from all targets and polarizations. This all inclusive acceptance ratio is defined as

$$\kappa_{two-target}=\frac{\sqrt[4]{a^{\uparrow}_{\text{up,Jura}}a^{\downarrow}_{\text{up,Saleve}}a^{\uparrow}_{\text{down,Jura}}a^{\downarrow}_{\text{down,Saleve}}}}{\sqrt[4]{a^{\uparrow}_{\text{up,Saleve}}a^{\downarrow}_{\text{up,Jura}}a^{\uparrow}_{\text{down,Saleve}}a^{\downarrow}_{\text{down,Jura}}}}. \qquad (1.10)$$

In this case the acceptance ratio is expected to vary less with time and therefore be closer to unity than the normal geometric mean acceptance ratio, Eq. 1.6. This is a consequence of having the different target cells oppositely polarized. Rewriting Eq. 1.10 with sub-period superscripts instead of target polarization superscripts

$$\kappa_{two-target} = \frac{\sqrt[4]{\mathrm{a}^a_{\mathrm{up,Jura}}\mathrm{a}^b_{\mathrm{up,Saleve}}\mathrm{a}^b_{\mathrm{down,Jura}}\mathrm{a}^a_{\mathrm{down,Saleve}}}}{\sqrt[4]{\mathrm{a}^a_{\mathrm{up,Saleve}}\mathrm{a}^b_{\mathrm{up,Jura}}\mathrm{a}^b_{\mathrm{down,Saleve}}\mathrm{a}^a_{\mathrm{down,Jura}}}}, \tag{1.11}$$

where sub-period a is with the upstream target polarized up and the downstream target polarized down and vise versa for sub-period b. From Eq. 1.11 it is more evident that the acceptance ratio terms for sub-period b are reciprocal to the terms for sub-period a and therefore the acceptance ratio is expected to be more stably close to unity.

Finally the statistical uncertainty of the two target geometric mean is

$$\frac{1}{\mathrm{P}}\frac{\mathrm{LR}}{\left(\mathrm{L+R}\right)^2}\sqrt{\sum_{\mathrm{target}}\sum_{\mathrm{polarization}}\left(\frac{1}{N^{\mathrm{polarization}}_{\mathrm{target,Left}}}+\frac{1}{N^{\mathrm{polarization}}_{\mathrm{target,Right}}}\right)} \quad, \tag{1.12}$$

where L can be thought of as the left counts and equals to $\sqrt[4]{N^\uparrow_{\mathrm{up,Left}}N^\downarrow_{\mathrm{up,Left}}N^\uparrow_{\mathrm{down,Left}}N^\downarrow_{\mathrm{down,Left}}}$ and R can be thought of as the right counts and equals $\sqrt[4]{N^\uparrow_{\mathrm{up,Right}}N^\downarrow_{\mathrm{up,Right}}N^\uparrow_{\mathrm{down,Right}}N^\downarrow_{\mathrm{down,Right}}}$. The statistical uncertainty for the two target geometric mean also reduces to $\frac{1}{\mathrm{P}}\frac{1}{\sqrt{\mathrm{N}}}$ in the case of equal statistics in each direction and polarization.
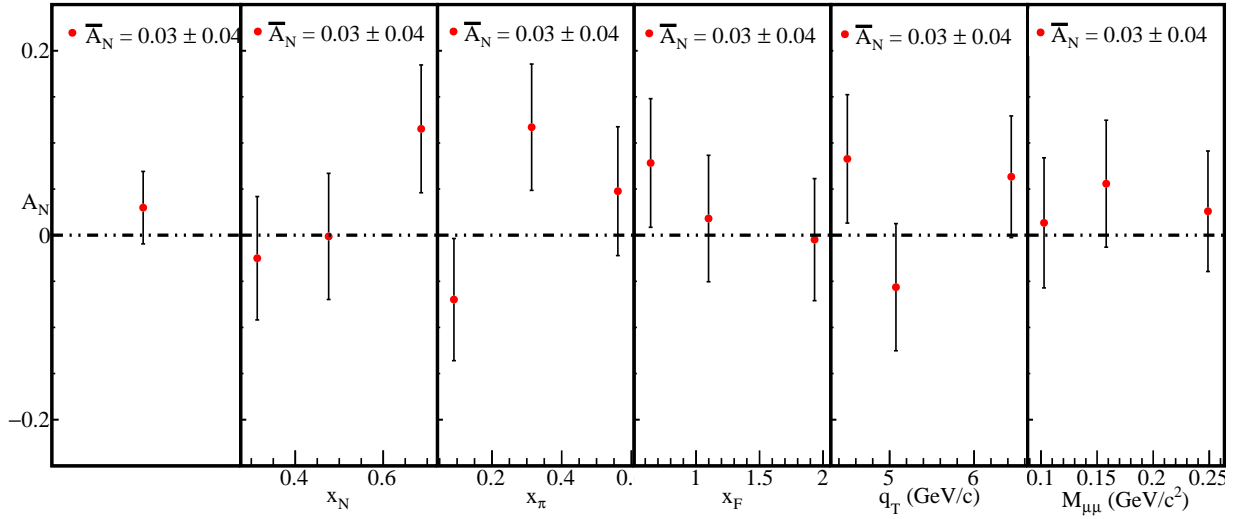
1.3 Results

The final asymmetries are calculated from each of the separate nine periods and then combined as a weighted average. This calculation method is used to minimize the effects of acceptance changes between periods as the spectrometer was kept stable within each period but had the options for detector changes and repairs between periods. This final asymmetry for each method is determined from a weighted average as

$$\mathrm{A_N} = \sum_{\mathrm{period}}\frac{\mathrm{A_{N,period}}\sigma^{-2}_{\mathrm{period}}}{\sigma^{-2}_{\mathrm{period}}}, \quad \sigma^2 = \sum_{\mathrm{period}}\frac{1}{\sigma^{-2}_{\mathrm{period}}}. \tag{1.13}$$

The final results for the basic geometric mean are shown in Fig. 1.1 and the final results for the two target geometric mean are shown in Fig. 1.2. The systematic error bars are discussed in Sec. 1.4.
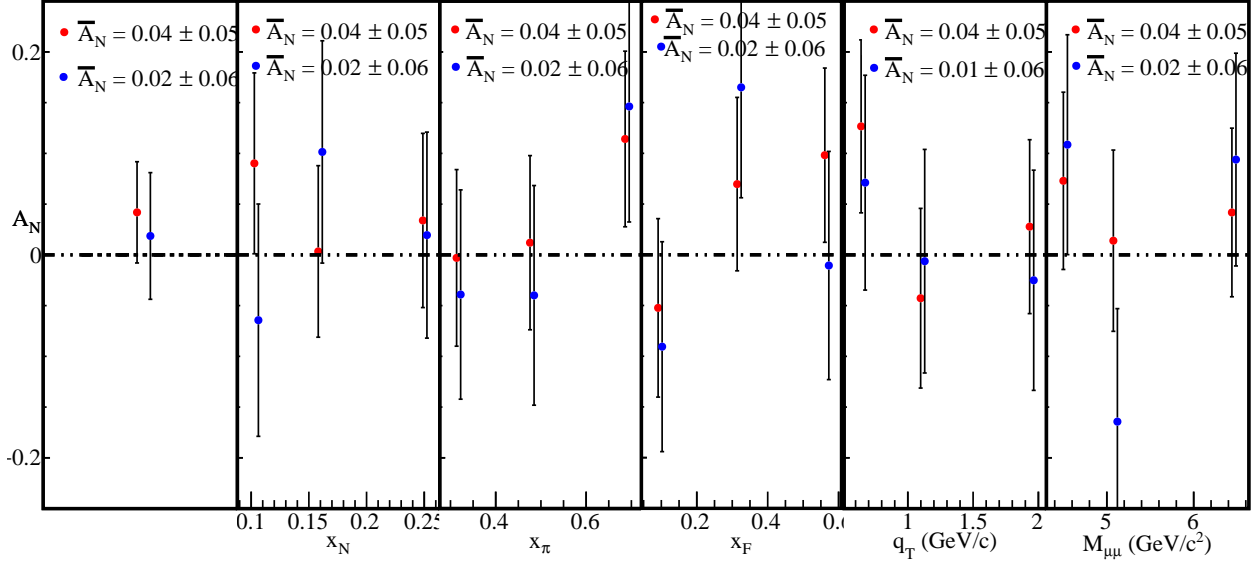
Figs 1.1 A_N determined from the geometric mean method for each target

Figs 1.2 A_N determined by the geometric mean method using both targets simultaneously

9

1.3.1 Comparison of results

1.4 Systematic Studies

Several tests were performed to estimate the systematic uncertainty. The final systematic errors are determined by adding all non-zero systematic effects in quadrature. The impact from each source of systematic error is summarized in Tab. 1.5.

1.4.1 Period Compatibility

The asymmetries calculated for each period in each kinematic bin are shown in Fig. 1.3.
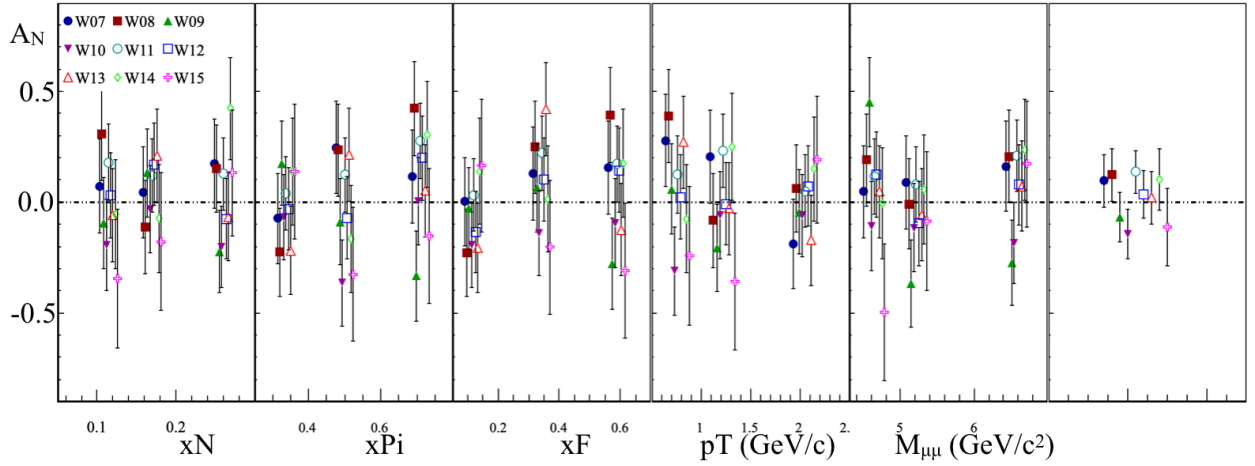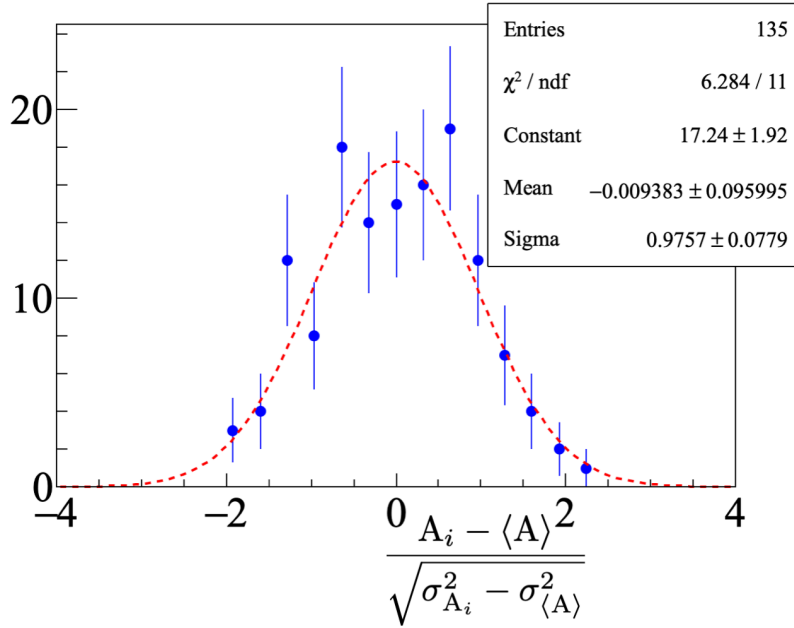

Figs 1.3 A_N determined for each period

By eye the asymmetry fluctuations appear to be statistically compatible. To quantify the compatibility of the asymmetries between the periods, a pull distribution is formed. The pull value is defined as

$$\Delta A_i = \frac{A_i - \langle A \rangle}{\sqrt{\sigma_{A_i}^2 - \sigma_{\langle A \rangle}^2}}, \tag{1.14}$$

and is determined for each period and kinematic bin. There are therefore 3(number of bins)x5(number of kinematics)x9(number of periods) = 135 entries in the pull distribution.
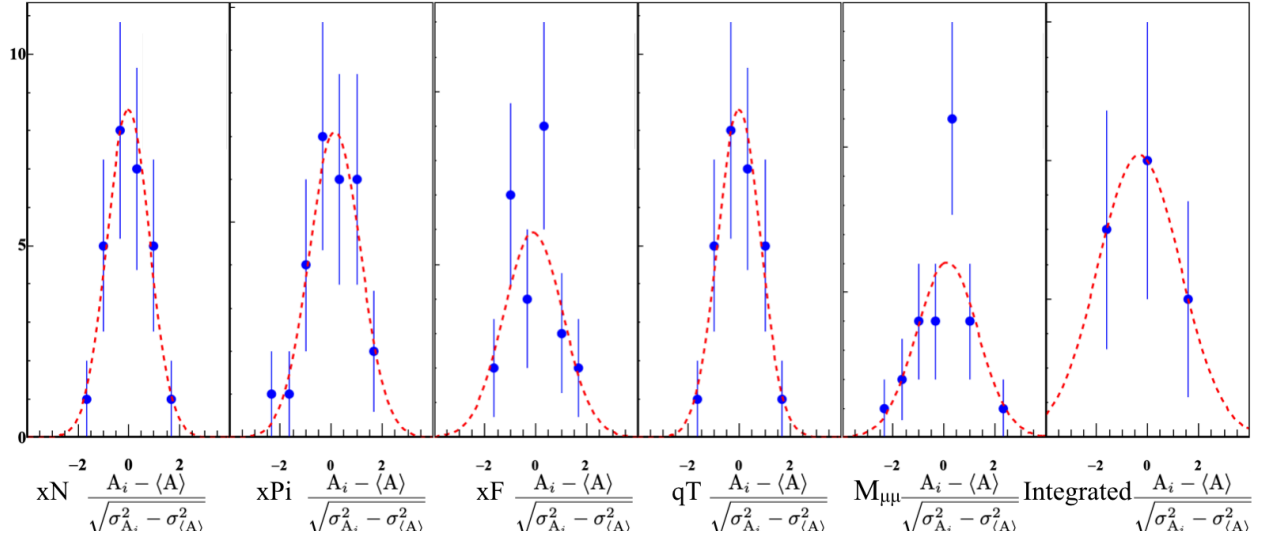
This distribution is shown in Fig. 1.4 along with a Gaussian fit. If the asymmetries all come from the same parent distribution then due to the central limit theorem the pull distribution will be a Gaussian distribution with zero mean and unit variance. The discrepancy of the pull distribution from a standard Gaussian distribution is used to determine a systematic error as

$$\frac{\sigma_{\text{systematic}}}{\sigma_{\text{statistical}}} = \sqrt{|\sigma_{\text{pull}}^2 - 1|} + \frac{\mu_{\text{pull}}}{2}. \tag{1.15}$$

Entries	135
χ^2 / ndf	6.284 / 11
Constant	17.24 ± 1.92
Mean	−0.009383 ± 0.095995
Sigma	0.9757 ± 0.0779

Figs 1.4 Pull distribution

As the asymmetries in different kinematic bins are formed using the same data set the asymmetries between kinematics are correlated. For this reason an uncorrelated pull distribution is also formed for each physics kinematic bin and also compared with a standard Gaussian distribution. These distributions are shown in Fig. 1.5 and the results of the Gaussian fit are shown in Fig. 1.6. For these uncorrelated pull distributions there are now only 3(number of bins)x9(number of periods) = 27 entries in each kinetically binned pull distributions and only 9(number of periods) bins in the integrated pull distribution.

Figs 1.5 Uncorrelated pull distributions

Entries	27
χ^2 / ndf	0.4347 / 3
Constant	8.548 ± 2.043
Mean	−0.01562 ± 0.17221
Sigma	0.8386 ± 0.1304

Entries	27
χ^2 / ndf	1.056 / 4
Constant	7.101 ± 1.827
Mean	0.1422 ± 0.2204
Sigma	1.004 ± 0.201

Entries	27
χ^2 / ndf	3.416 / 3
Constant	5.922 ± 1.622
Mean	−0.1036 ± 0.2910
Sigma	1.15 ± 0.31

Entries	27
χ^2 / ndf	0.4347 / 3
Constant	8.548 ± 2.043
Mean	−0.01562 ± 0.17221
Sigma	0.8386 ± 0.1304

Entries	27
χ^2 / ndf	3.152 / 4
Constant	6.038 ± 1.603
Mean	0.1287 ± 0.2860
Sigma	1.197 ± 0.256

Entries	9
χ^2 / ndf	1.091e−08 / 0
Constant	4.085 ± 1.992
Mean	−0.3308 ± 0.8192
Sigma	1.616 ± 1.101

Figs 1.6 Results of Gaussian fit for the uncorrelated pull distributions

Even though the Gaussian fits did not give exactly as standard Gaussian, the fit parameters well compatible with a standard Gaussian within the errors of the fit. Therefore no systematic error was assigned due to incompatibility of the periods.

1.4.2 False Asymmetries

Acceptance From False Asymmetries

As was pointed out in Sec. 1.2.1 and Sec. 1.2.2, the asymmetry measurement assumes the acceptance does not change with time and therefore the acceptance ratios Eq. 1.6 and Eq. 1.10 are unitary. Any deviation from a unitary acceptance ratio is estimated with a false asymmetry and the errors are included as systematic errors. To determine if acceptance does change with time, a false asymmetry is calculated where the only way the false asymmetry could be non-zero is if acceptance changes with time. This false asymmetry for the two target geometric mean is

$$
A_{\mathrm{N,False}} = \frac{1}{\mathrm{P}} \frac{\sqrt[4]{N^{\uparrow}_{\mathrm{up,Right}} N^{\downarrow}_{\mathrm{up,Left}} N^{\uparrow}_{\mathrm{down,Left}} N^{\downarrow}_{\mathrm{down,Right}}} - \sqrt[4]{N^{\uparrow}_{\mathrm{up,Left}} N^{\downarrow}_{\mathrm{up,Right}} N^{\uparrow}_{\mathrm{down,Right}} N^{\downarrow}_{\mathrm{down,Left}}}}{\sqrt[4]{N^{\uparrow}_{\mathrm{up,Right}} N^{\downarrow}_{\mathrm{up,Left}} N^{\uparrow}_{\mathrm{down,Left}} N^{\downarrow}_{\mathrm{down,Right}}} + \sqrt[4]{N^{\uparrow}_{\mathrm{up,Left}} N^{\downarrow}_{\mathrm{up,Right}} N^{\uparrow}_{\mathrm{down,Right}} N^{\downarrow}_{\mathrm{down,Left}}}}
$$

$$
= \frac{1}{\mathrm{P}} \frac{\alpha \sqrt[4]{\sigma_{Right}\sigma_{Left}\sigma_{Left}\sigma_{Right}} - \sqrt[4]{\sigma_{Left}\sigma_{Right}\sigma_{Right}\sigma_{Left}}}{\alpha \sqrt[4]{\sigma_{Right}\sigma_{Left}\sigma_{Left}\sigma_{Right}} + \sqrt[4]{\sigma_{Left}\sigma_{Right}\sigma_{Right}\sigma_{Left}}}
$$

$$
\tag{1.16}
$$

$$
= \frac{1}{\mathrm{P}} \frac{\alpha - 1}{\alpha + 1}, \tag{1.17}
$$

where α is an acceptance ratio and is defined as

$$
\frac{\sqrt[4]{a^{\uparrow}_{\mathrm{up,Saleve}} a^{\downarrow}_{\mathrm{up,Saleve}} a^{\uparrow}_{\mathrm{down,Jura}} a^{\downarrow}_{\mathrm{down,Jura}}}}{\sqrt[4]{a^{\uparrow}_{\mathrm{up,Jura}} a^{\downarrow}_{\mathrm{up,Jura}} a^{\uparrow}_{\mathrm{down,Saleve}} a^{\downarrow}_{\mathrm{down,Saleve}}}}. \tag{1.18}
$$

The false asymmetry, Eq. 1.16, can be simplified as

$$
A_{\mathrm{N,False}} = \frac{1}{\mathrm{P}} \frac{\sqrt[4]{N_{\mathrm{up,Saleve}} N_{\mathrm{down,Jura}}} - \sqrt[4]{N_{\mathrm{up,Jura}} N_{\mathrm{down,Saleve}}}}{\sqrt[4]{N_{\mathrm{up,Saleve}} N_{\mathrm{down,Jura}}} + \sqrt[4]{N_{\mathrm{up,Jura}} N_{\mathrm{down,Saleve}}}}. \tag{1.19}
$$

That is $A_{\mathrm{N,false}}$ is the normalized difference of counts from each target cell assuming the upstream target is always polarized down and the downstream target is always polarized up.

Given that the polarization flips for both upstream and downstream target cells, $A_{N,false}$ is an asymmetry where physical effects cancel out. The kinematic dependencies of the false asymmetry are shown in Fig. 1.7 and the kinematic dependencies of the acceptance ratio, α, are shown in Fig. 1.8.
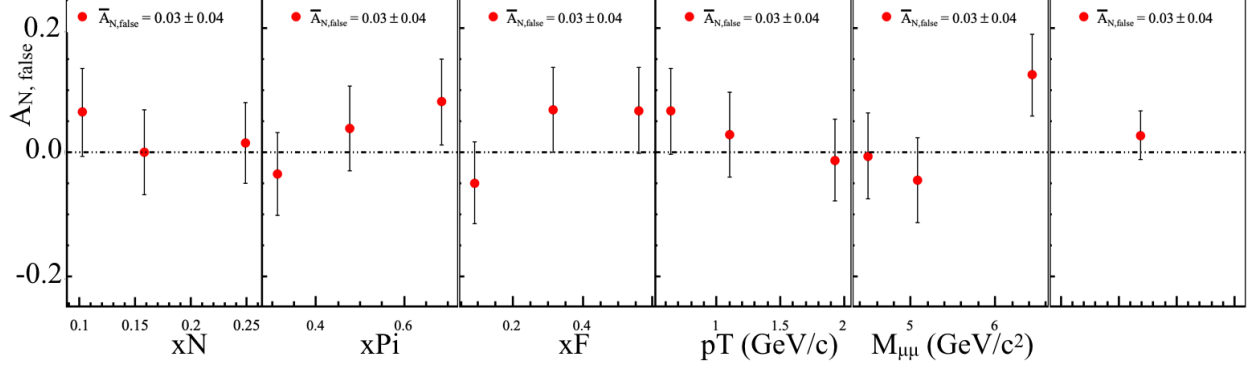
Figs 1.7 False asymmetry to estimate fluctuations in acceptance in time
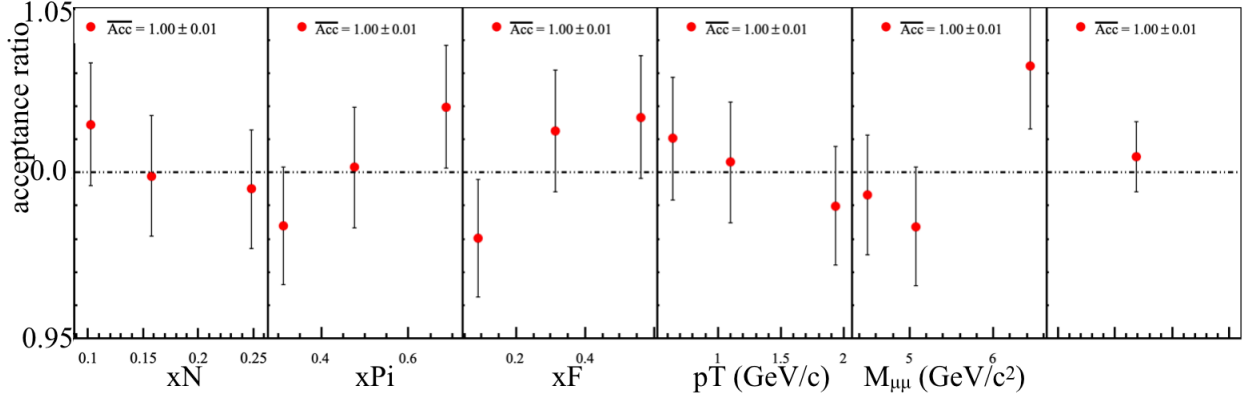

Figs 1.8 Acceptance ratio used to determine the systematic effects from acceptance changes in time

While α is an acceptance ratio it is not the same as the acceptance ratio in the true asymmetry. However α is similar to the true acceptance ratio, κ, in that α will only be different from unity as a result of time changes in the spectrometer. Therefore it is assumed α can be used as a good estimate of the true acceptance ratio fluctuations. The systematic error due to acceptance fluctuations is determined as

$$\delta A_{N,\text{systematic}} = \frac{1}{P}\left(\frac{|\alpha - 1|}{2} + \delta_{\frac{|\alpha-1|}{2}}\right), \tag{1.20}$$

where this expression is derived in Appendix A.1. The kinematic dependence of the systematic error normalized to the statistical error is shown in Fig. 1.9. The binned average systematic error due to acceptance is 20% of the statistical error.
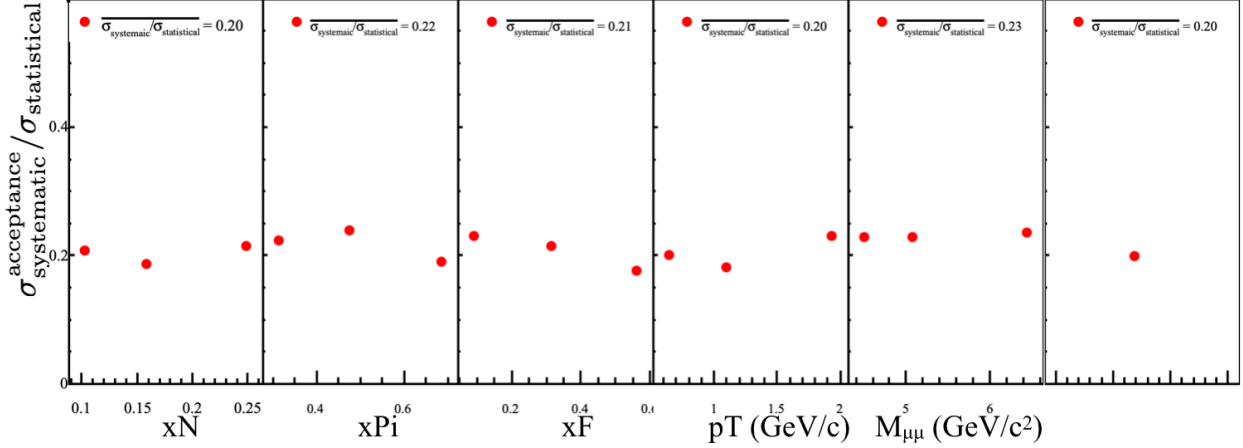
Figs 1.9 Systematic error due to acceptance effects

1.4.3 Further False Asymmetry Effects

Although the list of systematic effects specifically studied is quite exhaustive there is always the potential for other systematic effects not considered. Studies of the changes in time from additional false asymmetries were performed in an attempt to taken into account all other systematic effects. All false asymmetries considered must be constructed in such a way that the physical process of interest cancels out. A false asymmetry could therefore only be non-zero from acceptance effects, luminosity or some other reason not considered. The additional false asymmetries constructed are made in a way that luminosity effects canceled out and acceptance effects were approximately constant. With these assumptions pull values from Eq. 1.14 should be distributed as a standard Gaussian distribution. Any deviation from a standard Gaussian is conservatively taken as a systematic effect from some unknown cause.

The additional studied false asymmetries are summarized in the following enumerated list.

1. A false asymmetry similar to Eq. 1.16 but with the upstream left and right counts flipped defined as
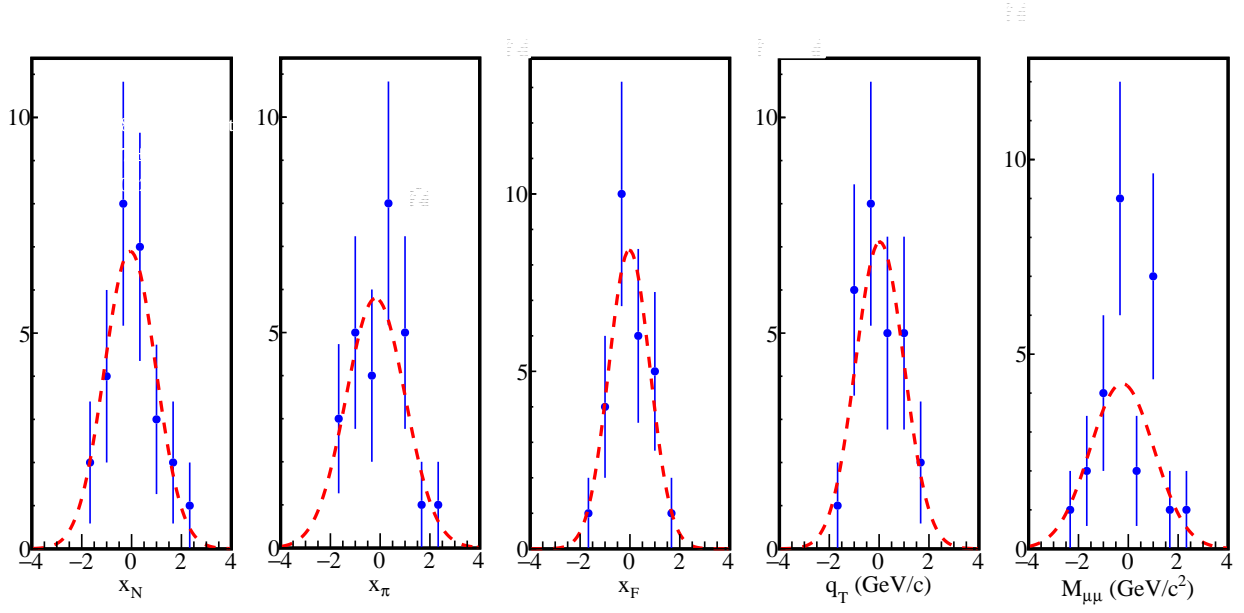
$$\frac{1}{P} \frac{\sqrt[4]{N^\uparrow_{\text{up,Left}} N^\downarrow_{\text{up,Right}} N^\uparrow_{\text{down,Left}} N^\downarrow_{\text{down,Right}}} - \sqrt[4]{N^\uparrow_{\text{up,Right}} N^\downarrow_{\text{up,Left}} N^\uparrow_{\text{down,Right}} N^\downarrow_{\text{down,Left}}}}{\sqrt[4]{N^\uparrow_{\text{up,Left}} N^\downarrow_{\text{up,Right}} N^\uparrow_{\text{down,Left}} N^\downarrow_{\text{down,Right}}} + \sqrt[4]{N^\uparrow_{\text{up,Right}} N^\downarrow_{\text{up,Left}} N^\uparrow_{\text{down,Right}} N^\downarrow_{\text{down,Left}}}}.$$
(1.21)

This false asymmetry can be thought of as measuring the normalized counts on the Jura side minus the Saleve side. The period weighted average results of this false asymmetry are shown in Fig. **??** and as can be seen there is the asymmetry is systematically less than zero by more than a standard deviation. The uncorrelated pull distributions from this false asymmetry are shown in Fig. 1.10 and the corresponding Gaussian fit results are shown in Fig. 1.11. Due to the fact that there are less entries in these pull distributions the Gaussian fit results are not necessarily that good. In an attempt to correct for this and to take into account the fit errors, a weighted average of the mean and standard deviation are made, as in Eq. 1.13, using weights as the inverse fit variances. The final systematic error is again determined as in Eq. 1.15 using the weighted mean and weighted standard deviation.

2. A false asymmetries using only the information from the upstream or the downstream target defined as

$$\frac{1}{P} \frac{\sqrt{N^\uparrow_{\text{up(down)stream,Left}} N^\downarrow_{\text{up(down)stream,Right}}} - \sqrt{N^\uparrow_{\text{up(down)stream,Right}} N^\downarrow_{\text{up(down)stream,Left}}}}{\sqrt{N^\uparrow_{\text{up(down)stream,Left}} N^\downarrow_{\text{up(down)stream,Right}}} + \sqrt{N^\uparrow_{\text{up(down)stream,Right}} N^\downarrow_{\text{up(down)stream,Left}}}}.$$
(1.22)

This false asymmetry can also be thought of as measuring the normalized counts on the Jura side minus the Saleve side but for each target individually. Both this false
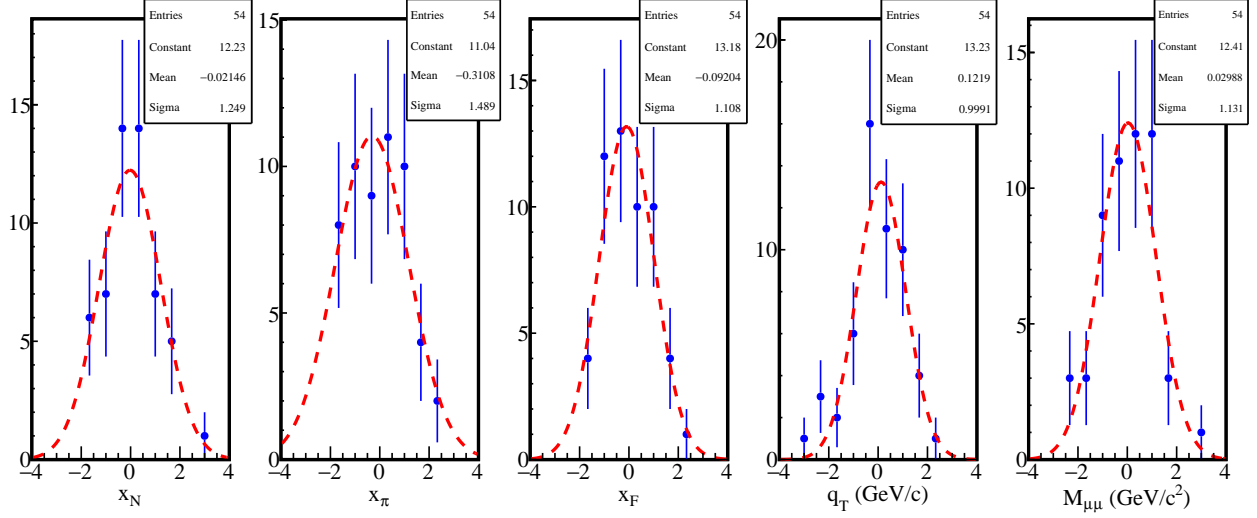
Figs 1.10

Entries	27	Entries	27	Entries	27	Entries	27	Entries	27
χ^2 / ndf	1.06 / 4	χ^2 / ndf	2.875 / 4	χ^2 / ndf	1.203 / 3	χ^2 / ndf	1.925 / 3	χ^2 / ndf	7.364 / 5
Constant	6.898 ± 2.019	Constant	5.797 ± 1.578	Constant	8.419 ± 2.089	Constant	7.116 ± 1.826	Constant	4.248 ± 1.307
Mean	-0.05617 ± 0.22189	Mean	-0.1796 ± 0.3545	Mean	-0.02243 ± 0.17361	Mean	0.0256 ± 0.2382	Mean	-0.2528 ± 0.3265
Sigma	1.032 ± 0.266	Sigma	1.187 ± 0.317	Sigma	0.8256 ± 0.1377	Sigma	0.9721 ± 0.1962	Sigma	1.279 ± 0.331

Figs 1.11

asymmetry and the previous false asymmetry can be written as Eq. 1.17 where α will be an acceptance ratio of Jura/Saleve. As the Jura/Saleve acceptance ratio is expected to be the same for the upstream and downstream targets, any difference between the two false asymmetries must be due to other reasons. A by period comparison between the upstream and downstream target is shown in Fig. **??** and as can be seen there are difference by period between the upstream and downstream asymmetries. A combined

17

pull distribution is made using the information from both upstream and downstream asymmetries and is shown in Fig. 1.12. As with the previous false asymmetry, lack of data leads to the same problems with fit and therefore the same weighting method is used to determine a systematic error.
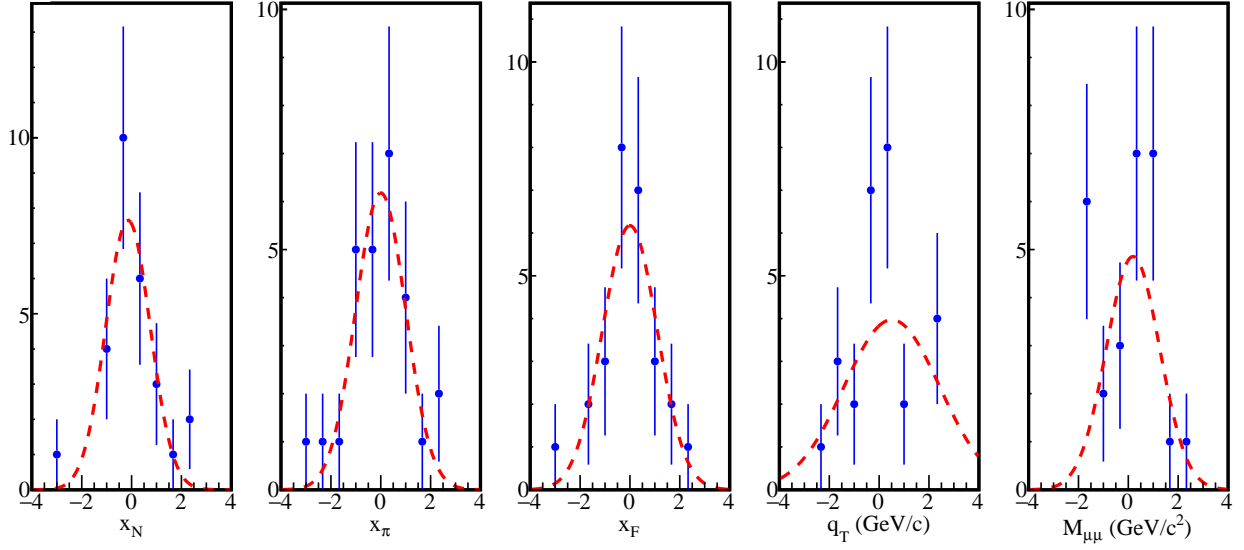

Figs 1.12

3. Finally the same false asymmetry used to determine the acceptance fluctuations, Eq. 1.16, is also checked for compatibility and a systematic error is determined in the same way as the previous false asymmetries. The pulls are shown in Fig. 1.13 and the corresponding fit parameters are shown in Fig. 1.14.

A summary of the systematic error from each false asymmetry is shown in Tab. 1.4

Systematic error	$\langle \sigma_{\text{systematic}} / \sigma_{\text{statistical}} \rangle$
2 Target	0.0
Acceptance fluctuation	0.2
Total	0.0

Table 1.4 Summary of systematic error impacts from false asymmetries. The maximum systematic error is chosen as the final systematic error.

Figs 1.13

		Entries	27							
		χ^2 / ndf	3.517 / 4							
		Constant	7.658 ± 3.014							
		Mean	−0.1441 ± 0.2765							
		Sigma	0.891 ± 0.424							

		Entries	27
		χ^2 / ndf	3.737 / 6
		Constant	6.183 ± 1.859
		Mean	−0.002351 ± 0.211941
		Sigma	1.004 ± 0.226

		Entries	27
		χ^2 / ndf	2.357 / 5
		Constant	6.176 ± 2.115
		Mean	−0.002406 ± 0.246275
		Sigma	1.098 ± 0.361

		Entries	27
		χ^2 / ndf	6.734 / 4
		Constant	3.971 ± 1.201
		Mean	0.5095 ± 1.1086
		Sigma	1.92 ± 1.12

		Entries	27
		χ^2 / ndf	7.973 / 4
		Constant	4.857 ± 4.667
		Mean	0.1882 ± 0.9446
		Sigma	1.072 ± 1.195

Figs 1.14

1.4.4 Left/Right Event Migration

The spectrometer has finite resolution for any measured quantity and for this reason events measured as left outgoing could really be events that are right outgoing and vise versa for measured left outgoing events. This left-right miss-identification has the result of diluting spin-dependent effects by effectively having a sample from an unpolarized target along with the sample from the polarized target. Therefore the asymmetry A_N reduces from left-right

miss-identification and this effect is included as a systematic effect.

Miss-identification was estimated from a simulated Monte-Carlo data sample where the sample was made from the respond of the COMPASS spectrometer to input Drell-Yan events in a similar mass range. The same analysis performed on real data was performed on this Monte-Carlo data to get the angles of interest. Fig. **??** shows the rate of events identified correctly and incorrectly as a function of the ϕ_S. This plot is made by determining which outgoing direction the generated events emerged with the outgoing direction the reconstructed events emerged.

As is clearly visible there is a band of higher miss-identification rate at the border between left and right. For this reason a cut in the ϕ_S variable symmetric about the left-right border was tested to determine the percent of miss-identification as a function of the amount of ϕ_S cut. These results are shown in Fig. **??**.

The systematic error for left-right migration is calculated as

$$\delta A_{N,\text{systematic}} = \gamma * A_N + \gamma * \delta A_N, \tag{1.23}$$

where this expression is derived in Appendix A.2.

The systematic error normalized to the statistical error as a function of the amount of ϕ_S cut is shown in Fig. **??**. No cut on ϕ_S was used for the final asymmetry due to the fact that the systematic error is already small with no cut in ϕ_S and to avoid loss of statistics. The final systematic error due to left-right event migration was determined to be 5% of the statistical error and add in quadrature per physics bin.

Systematic error	$\langle \sigma_{\text{systematic}}/\sigma_{\text{statistical}} \rangle$
Period compatibility	0.0
Acceptance fluctuation	0.2
Total	0.0

Table 1.5 Summary of systematic error impacts to the integrated asymmetry

Appendix A

A.1 Systematic Error From Acceptance

For an asymmetry defined as

$$A_\alpha = \frac{1}{P} \frac{\alpha\sigma_L - \sigma_R}{\alpha\sigma_L + \sigma_R} \tag{A.1}$$

where α is an acceptance ratio. α is assumed to be close to unity therefore let

$$\alpha = 1 \pm 2 * \epsilon, \tag{A.2}$$

where ϵ is a small positive number. The asymmetry can therefore be written

$$\frac{1}{P} \frac{(1 \pm 2 * \epsilon)\sigma_L - \sigma_R}{(1 \pm 2 * \epsilon)\sigma_L + \sigma_R} = \frac{1}{P} \frac{\sigma_L - \sigma_R \pm 2 * \epsilon * \sigma_L}{(\sigma_L + \sigma_R)(1 \pm \frac{2*\epsilon*\sigma_L}{\sigma_L + \sigma_R})}. \tag{A.3}$$

From there Taylor expand the denominator to get

$$A_\alpha \approx \frac{1}{P} \frac{\sigma_L - \sigma_R \pm 2 * \epsilon * \sigma_L}{(\sigma_L + \sigma_R)} * (1 \mp \frac{2 * \epsilon * \sigma_L}{\sigma_L + \sigma_R}) \tag{A.4}$$

$$= A_N \pm \frac{1}{P} \frac{2 * \epsilon * \sigma_L}{\sigma_L + \sigma_R} \mp A_N * \frac{2 * \epsilon * \sigma_L}{\sigma_L + \sigma_R} \mp \frac{1}{P} \left(\frac{2 * \epsilon * \sigma_L}{\sigma_L + \sigma_R}\right)^2.$$

Assuming A_N is small and $\sigma_L \approx \sigma_R$

$$A_\alpha \approx A_N \pm \frac{\epsilon}{P}. \tag{A.5}$$

The true asymmetry can now be written

$$A_{N,\text{systematic}} \approx A_\alpha \mp \frac{\epsilon}{P}. \tag{A.6}$$

Including the $\frac{\epsilon}{P}$ term as an additive error and using standard error propagation the systematic error can be approximated as

$$\delta A_{N,\text{systematic}} = \frac{\mid \alpha - 1 \mid}{2} \frac{1}{P} + \frac{\delta_{\frac{\mid\alpha-1\mid}{2}}}{P}. \tag{A.7}$$

A.2 Systematic Error From Left-Right Event Migration

Assuming the fraction of events miss-identified is γ and that the amount of miss-identified events reconstructed left equals the amount of outgoing events reconstructed right

$$A_{N,\text{measure}} = \frac{1}{P} \frac{(L + \frac{\gamma}{2}N_{\text{total}}) - (R + \frac{\gamma}{2}N_{\text{total}})}{(L + \frac{\gamma}{2}N_{\text{total}}) + (R + \frac{\gamma}{2}N_{\text{total}})} = \frac{1}{P} \frac{L - R}{(L + R) * (1 + \gamma * \frac{N_{\text{total}}}{L+R})}, \tag{A.8}$$

where N_{total} is the total events measure, L is the true events measured to the left that should be measured left and R is the number of events measure to the right that should be measured to the right.

Assuming γ is a small percentage, the denominator can be Taylor expanded to give

$$A_{N,\text{measure}} \approx A_N \left(1 - \gamma * \frac{N_{\text{total}}}{L + R} \right). \tag{A.9}$$

Including $\gamma A_{N,\text{measure}}$ as an additive error and using standard error propagation the systematic error can be approximated as

$$\delta A_{N,\text{systematic}} = \gamma * A_{N,\text{measure}} + \gamma * \delta A_{N,\text{measure}}. \tag{A.10}$$

List of Figures

List of Tables

listed in References

Appendix B

References